Investigation of mechanical properties of soft hydrogel microcapsules in relation to protein delivery using a MEMS force sensor

Keekyoung Kim,[1] Ji Cheng,[2] Qun Liu,[2] Xiao Yu Wu,[2] Yu Sun[1]
[1]*Advanced Micro and Nanosystems Laboratory, University of Toronto, 5 King's College Road, Toronto, Ontario, Canada M5S 3G8*
[2]*Leslie Dan Faculty of Pharmacy, University of Toronto, 144 College Street, Toronto, Ontario, Canada M5S 3M2*

Received 30 May 2008; revised 31 August 2008; accepted 22 September 2008
Published online 22 January 2009 in Wiley InterScience (www.interscience.wiley.com). DOI: 10.1002/jbm.a.32338

Abstract: This article reports the investigation of mechanical properties of alginate–chitosan microcapsules and the relation to protein delivery. For microscale compression testing, a system based on a microelectromechanical systems (MEMS) capacitive force sensor was developed. The bulk microfabricated capacitive force sensors are capable of resolving forces up to 110 μN with a resolution of 33.2 nN along two independent axes. The monolithic force sensors were directly applied to characterizing mechanical properties of soft hydrogel microparticles without assembling additional end-effectors. Protein-loaded alginate–chitosan microcapsules of ~20 μm in diameter were prepared by an emulsion-internal gelation-polyelectrolyte coating method. Young's modulus values of individual microcapsules with 1, 2, and 3% chitosan coating were determined through microscale compression testing in both distilled deionized (DDI) water and pH 7.4 phosphate-buffered saline (PBS). Protein release rates were also determined in DDI water and PBS. Finally, protein release rates were correlated with mechanical properties of the microcapsules. © 2009 Wiley Periodicals, Inc. J Biomed Mater Res 92A: 103–113, 2010

Key words: alginate–chitosan microcapsules; MEMS force sensors; microscale compression test; Young's modulus; protein release rate

INTRODUCTION

Hydrogel microcapsules have been widely used for the controlled delivery of therapeutic agents (e.g., protein drugs) and the encapsulation of living cells because of their hydrophilic nature resembling living tissues and, thereby, high biocompatibility. Owing to their capability of holding a large quantity of water, hydrogel microcapsules provide an environment suitable for stabilizing proteins, which readily denature at hydrophobic interfaces.

Hydrogel microcapsules are highly deformable with diameters typically ranging from 1 to 100 μm, comparable to most biological cells. When they are used for drug delivery or cell encapsulation, their mechanical strength determines whether they can survive the stress in the needle tract during injection, in the blood capillaries, or in the applied tissues. Maintaining their integrity during processing and application is essential for the prevention of dose dumping and cell death and/or immunoresponse as well as for providing desired performance. On the other hand, their mechanical strength is related to solute permeation because of its dependence on the hydration degree of the hydrogel, which influences the release of therapeutic agents and diffusion of cell nutrients and metabolites. Since the hydration degree of hydrogels is a function of polymer composition, cross-linking density, and environmental conditions such as medium pH and ionic strength, it is conceivable that the mechanical properties of hydrogel microcapsules also depend on these material and environmental parameters. Quantitative characterization of mechanical properties of hydrogel microcapsules can therefore help guide the rational design of this unique drug and cell delivery system.

As a soft, microscale material, however, individual hydrogel microcapsule's mechanical properties are difficult to characterize quantitatively, requiring a system that is capable of accurately measuring low-magnitude forces and microscopic material deforma-

Correspondence to: Y. Sun; e-mail: sun@mie.utoronto.ca
Contract grant sponsors: Natural Sciences and Engineering Research Council of Canada, Ontario Ministry of Research and Innovation

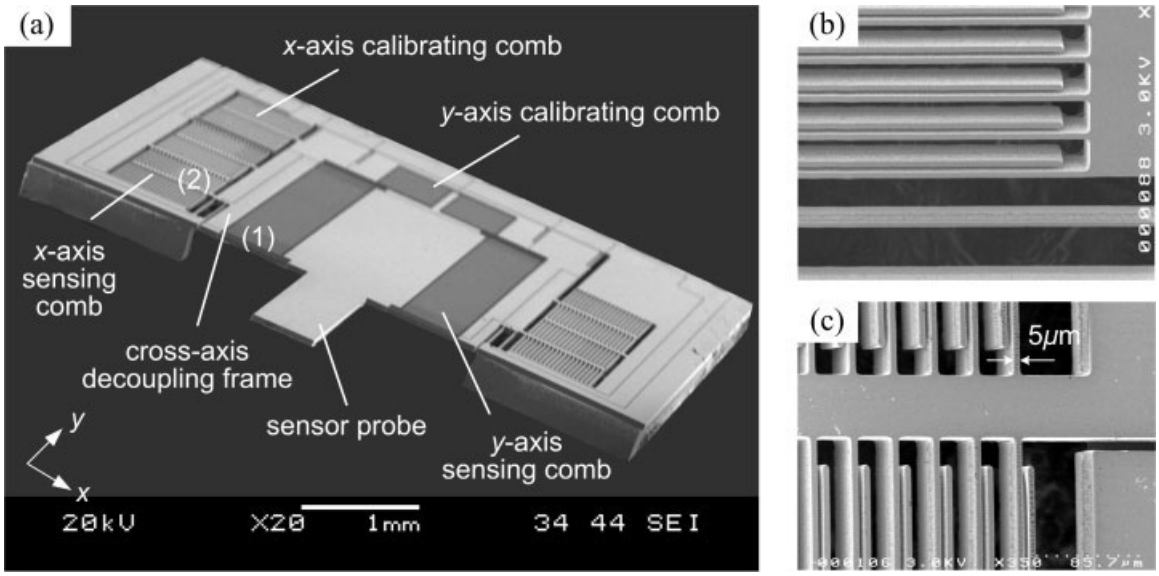

Figure 1. SEM images of (a) a capacitive force sensor. (b, c) Zoom-in views of areas (1) and (2) labeled in (a).

tions. Existing techniques for biomaterial mechanical characterization, such as micropipette aspiration,[1] atomic force microscopy (AFM),[2,3] and magnetic bead measurement[4] are limited to local probing for quantifying local mechanical parameters of biomaterials. Therefore, efforts have been spent to develop techniques for globally compressing microscale biomaterials between two plates. A micromanipulation system integrating a commercially available force transducer was developed for quantifying bursting forces of single biological cells,[5–7] bursting forces and Young's modulus of microcapsules,[8–10] adhesive forces of poly(methylidene malonate 2.12) microparticles,[11] and mechanical parameters of gelatin-rich microparticles.[12] AFM tip with an assembled colloid sphere has also been demonstrated as a microscale compression testing tool for characterizing the Young's modulus of polyelectrolyte multilayer microcapsules[13,14] and Jurkat T-lymphoma cells.[15]

However, the aforementioned microscale compression techniques require additional side view microscopes to measure the deformation of biomaterials, making the experimental setup complex. Moreover, assembling end-effectors, such as an optical fiber probe to a commercial force transducer or a colloid sphere to an AFM tip, requires additional elaborate efforts. The assembly of end-effectors is time consuming and, more importantly, can result in nonuniformity (alignment errors) in device configurations.

Microelectromechanical system (MEMS) devices are useful tools for investigating mechanical properties of microscale biomaterials because of their advantages such as wide force measurement ranges with high resolutions and the capability of direct application to mechanical characterization of biomaterials as monolithic devices without the need of assembling end-effectors. MEMS piezoresistive force sensors have been demonstrated for the measurement of contractile forces of individual heart cells.[16] Micromachined optical force sensors were developed to measure the injection force of drosophila embryos.[17] MEMS force sensor based on flexible beams for studying cell mechanics[18] and polydimethylsiloxane (PDMS) pillar array for cellular force measurements[19] were also reported. MEMS capacitive force sensors were demonstrated for characterizing mechanical properties of mouse oocytes/embryos[20] and for characterizing the flight behavior of fruit flies.[21]

Different from the designs reported by Sun et al.,[20,21] the capacitive force sensors (Fig. 1) presented in this article have much improved performance, providing a high force measurement resolution, highly linear response along two axes, matched sensitivity along both axes, and minimized cross-axis coupling. The capacitive force sensors are capable of resolving both normal and tangential forces in the range of [10^{-6} N, 10^{-9} N]. These MEMS capacitive force sensors were applied to microscale compression testing of individual microcapsules and produced useful data for selecting materials and formulations of microcapsules.

In this study, the mechanical properties of alginate microcapsules coated with chitosan were characterized. The alginate–chitosan microcapsules were developed for protein immobilization, which provided prolonged bioactivity of glucose oxidase.[22] Alginate, as a natural hydrogel material, is one of the most popular polymers used for cell encapsulation owing to its high biocompatibility.[23,24] Alginate-based microparticles can be prepared under a mild condition at room temperature without the use of or-

ganic solvents. The relatively inert aqueous environment inside the gel, a controllable gel porosity by coating with polycationic polymers (e.g., chitosan), and degradability under physiological conditions make alginate an excellent material for protein delivery. Alginate microcapsules have been studied for sustained release or immobilization of bioactive agents such as enzymes,[25] vaccine,[26] insulin,[27] and cytokines.[28,29]

In a previous work by Liu et al.,[22] an internal gelation-protein-adsorption-polyelectrolyte coating method was employed. This method was designed to avoid the contact of protein with hydrophobic interfaces thus preventing protein denaturation. Calcium alginate gel microcapsules were first prepared, washed, and then incubated with protein aqueous solutions. Following protein adsorption, the microcapsules were coated with a cationic polymer such as chitosan by polyelectrolyte complexation.[22,30–33] It was found that chitosan coating could stabilize immobilized protein and reduce permeability and loading efficiency depending on the concentration of chitosan solution, incubation time and pH. It is speculated that chitosan coating would also affect the mechanical properties of the microcapsules because of the formation of alginate–chitosan complexes, the control of which can be utilized to achieve desired release rates of therapeutic agents while fulfilling the requirement for essential mechanical properties.

This work was aimed at quantitative characterization of Young's modulus values of individual alginate–chitosan microcapsules at wet state in both distilled deionized (DDI) water and pH 7.4 phosphate-buffered saline (PBS) using the MEMS capacitive force sensors. The release rates of protein from the microcapsules with 1, 2, and 3% chitosan coating were determined and correlated to their mechanical properties.

MATERIALS AND EXPERIMENTAL METHODS

Preparation of alginate–chitosan microcapsules

Alginate sodium salt of medium molecular weight (viscosity of 2.0% solution 3500 cps at 25°C) was purchased from Sigma (St. Louis, MO). Ultrafine calcium carbonate powder (Miltifex-MM, 0.074 μm) was donated by Special Minerals (Adams, MA). Chitosan was purchased from Fluka (Buchs, SG, Switzerland) and modified before use by a free radical degradation method. PBS of pH 7.4 (~0.156*M*) was purchased from Invitrogen (Burlington, ON, Canada). DDI water was prepared by a Millipore (Billerica, MA) system.

A method reported by Liu et al.[22] was modified to prepare GOx-loaded alginate–chitosan microcapsules of 20 μm in mean diameter. In brief, the ultrafine calcium carbonate powder was dispersed in an alginate solution and emulsified in light mineral oil containing Span 80 under stirring. Gelation was initiated by the addition of acetic acid. The resultant microcapsules were recovered by centrifugation. Then 500 μL of microcapsules were added into 500 μL of 500 μg/mL GOx in pH 4 acetate buffer. The adsorption experiments were conducted for 30 min at 4°C, followed by incubation of the GOx-loaded microcapsules in chitosan solutions of different concentrations (1, 2, 3%, w/v) in 0.3% (v/v) acetic acid for 10 min. Finally, the microcapsules were rinsed with 10 mL of DDI water for three times to remove unencapsulated GOx.

Experimental method for mechanical property characterization

MEMS force sensors

The capacitive MEMS force sensors employed bulk-micromachined, transverse differential comb drives for achieving a high sensitivity and linearity, and two separated, movable inner and outer frames for suppressing cross-axis coupling. Applied forces along the x or y direction respectively deflect eight unidirectional springs and further change comb finger gaps. The total capacitance change resolves an applied force. The springs are orthogonally configured with movable inner and constrained outer frames to decouple force sensing along the x and y directions. The eight springs are modeled as a fixed-guided beam with a point load applied at the end of the beam. The applied force along the x or y direction is

$$F_{x,y} = \frac{8Etw^3\Delta d_{x,y}}{l^3} \tag{1}$$

where $\Delta d_{x,,y}$ is the deflection of beams which results in the displacement of movable comb fingers, $E = 160$ GPa is the average Young's modulus of p-type $\langle 100 \rangle$ silicon, and l, w, and t are spring length, width, and thickness. To achieve a high sensitivity and linear input–output relationship, transverse tri-plate differential comb drives shown in Figure 2 are used.[21] When a force F_y is transmitted to the y directional force sensor, movable comb set 2 in Figure 2(b) moves away from stationary comb set 3 and closer to stationary comb set 1. The gaps between comb fingers become $d_{y1} = d_0 - \Delta d_y$, $d_{y2} = d_0' + \Delta d_y$, $d_{y3} = d_0 + \Delta d_y$, and $d_{y4} = d_0' - \Delta d_y$, where d_0 and d_0' are initial gaps. Then, capacitances are

$$C_{y1} = n\frac{K\varepsilon_0 tl}{d_{y1}} + n\frac{K\varepsilon_0 tl}{d_{y2}}, \quad C_{y2} = n\frac{K\varepsilon_0 tl}{d_{y3}} + n\frac{K\varepsilon_0 tl}{d_{y4}} \tag{2}$$

where K is the dielectric constant for air, ε_0 is the permittivity of free space, $t \times l$ is the overlapping area of comb fingers, and n is the number of comb finger pairs. Capacitance changes and corresponding voltage changes are measured through a readout system by

$$V_{\text{out}-y} = V_{\text{ref}}\left(\frac{C_{y1} - C_{y2}}{C_{y1} + C_{y2}}\right) = V_{\text{ref}}\left(\frac{\Delta d_y d_0' - \Delta d_y d_0}{d_0 d_0' - \Delta d_y{}^2}\right) \cong V_{\text{ref}}\left(\frac{\Delta d_y}{d_0}\right) \tag{3}$$

By initially setting $d_0 \ll d_0'$, the resulting output signal $V_{\text{out-}y}$ as well as the applied force F_y are proportional to the

middle-plate displacement Δd_y. Therefore, the undesired additional capacitive effect can be minimized by placing repeated comb-plate units reasonably far apart (e.g., $d_0 = 5$ μm and $d_0' = 20$ μm used in this design). In this reported design, when $\Delta d_y < 2$ μm, input–output linearity is better than 1.5%. The above analysis is also applicable to the x direction. Structural electrostatic coupled finite element simulation was conducted to determine spring dimensions and the placement of comb drives to maximize sensitivity while minimizing cross-axis coupling and nonlinearity.

The high-aspect-ratio sensors were constructed through a high-yield DRIE-SOI process, modified from the process presented by Sun et al.[34] The process etches both handle (500 μm thick) and device (50 μm thick) Si layers, permits electrical isolation and mechanical connection, creates a step difference on suspended movable frames to enhance device robustness for handling, and enables dice free device release.

The force sensors were calibrated by actuation combs connected to force sensing combs in the x and y directions. The dedicated actuation comb drives for self-calibration facilitates the calibration process without damaging the small, fragile microdevices. Calibration was conducted under a probe station. Actuation voltages were applied through a DC power supply. Corresponding images were taken by a digital camera mounted on the probe station. Simultaneously, output voltages from force sensing comb were sampled through a data sampling program. Gap distances between actuation comb fingers were measured through the images with a resolution of 0.032 μm/pixel. Actuation forces were calculated by

$$F_{\text{actuation}} = \frac{V^2 n \varepsilon_0 t l}{2 (d_0 - \Delta d)^2} \quad (4)$$

where V is the applied actuation voltage, n is the number of comb drives, ε_0 is the permitivity of free space, $t \times l$ is the overlapping area of comb fingers, d_0 is the initial gap distance, and Δd is the gap displacement caused by electrostatic actuation. Figure 3 shows the calibration results of the force sensors along both x and y directions, demonstrating a highly linear relationship between applied forces and voltage changes and suppressed cross-axis coupling. The MEMS capacitive force sensors are capable of resolving forces up to 110 μN with a resolution of 33.2 nN along both axes (in plane).

System setup

Figure 4(a,b) shows the experimental system setup, and Figure 4(c) illustrates the experimental situation where a microcapsule is held by a low suction pressure through a PDMS channel. A droplet of DDI water or pH 7.4 PBS containing suspended alginate–chitosan microcapsules (ranging from 15 to 25 μm) was dispensed through pipetting on a glass slide with a bonded multichannel PDMS holding device. A syringe pump (Pico Plus, Harvard Apparatus) applied a low suction pressure to hold alginate–chitosan microcapsules through 4 μm channels of the PDMS holding device, and a microrobot controlled the force sensor to immerse the sensor probe into the liquid droplet and conducted compression testing.

The system included a 3-DOF microrobot (MP-285, Sutter) for positioning the force sensor, an inverted microscope (IX81, Olympus) with a CMOS camera (A601f, Basler), and a MEMS capacitive force sensor wire-bonded to a custom designed readout circuit which was built around an ASIC (AD7746, Analog Devices) for measuring capacitance changes. All the components except the host computer were mounted on a vibration isolation table. The horizontally aligned force sensor probe (3 mm long) was capable of reaching and compressing the alginate–chitosan microcapsules inside liquid medium against the PDMS wall without immersing the comb drives into the medium.

Force measurements along the tangential direction (x direction) were used in experiments for the proper alignment of the force sensor probe with a microcapsule. Forces along the normal direction (y direction) and image data were synchronously acquired by a custom-built data acquisition program. Figure 5 is a series of snapshots from the experiments. The force sensor controlled by the microrobot continuously compressed individual alginate–chitosan microcapsules up to 20% of deformation with a compression speed of 1.25 μm/s.

Experimental method for GOx release test

The GOx release test was conducted using 0.5 mL of GOx alginate–chitosan microcapsules in 10 mL of pH 7.4 PBS or DDI water at 37°C. The concentration of GOx in the buffer solution was measured by a BioRad protein microassay (Hercules, CA). Briefly, an 800 μL sample was taken at different time intervals (1, 3, 5, 8 h), 200 μL of assay solution was added, the mixture was incubated at room temperature for 10 min, and the ultraviolet absorption of the mixture at 596 nm was measured. After each sampling, an 800 μL of the fresh buffer was added to the testing medium.

Statistical analysis

Each experiment was repeated three times for drug release testing and five times for compression testing. The results were expressed as means ± SD. The analysis of variance was applied to compare the effect of chitosan coating on the mechanical properties and the GOx release kinetics. A value of $p < 0.05$ was considered statistically significant.

RESULTS AND DISCUSSION

Mechanical characterization of Young's modulus

From microscale compression testing, compressive forces and displacements data were collected simultaneously via force sensing signal and corresponding microscopic image data. To quantify Young's modulus values, the force–displacement data were assessed by a mechanics model.

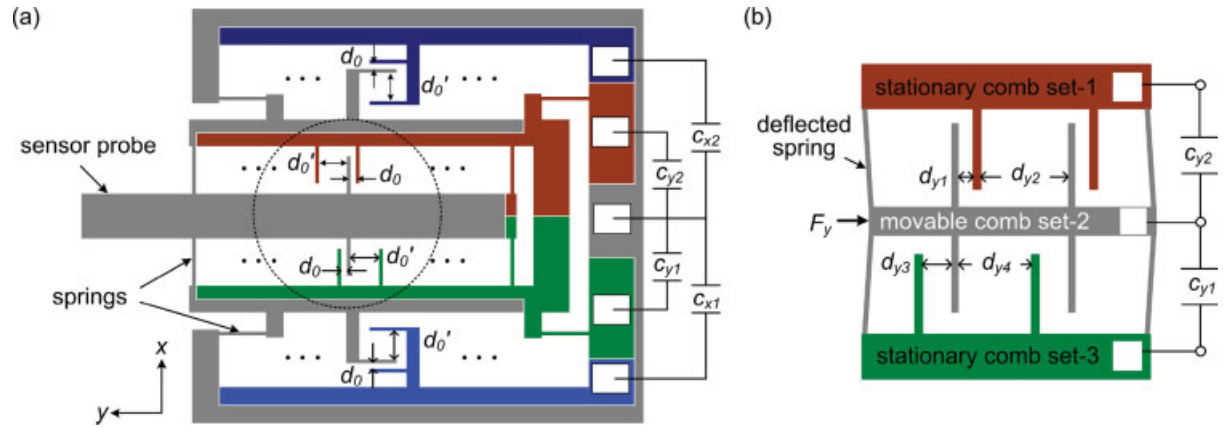

Figure 2. Schematics of a capacitive force sensor. (a) Initial state in x and y directions. (b) Zoom-in view of a tri-plate comb in a dotted circle, when a force F_y is applied to the sensor probe. [Color figure can be viewed in the online issue, which is available at www.interscience.wiley.com.]

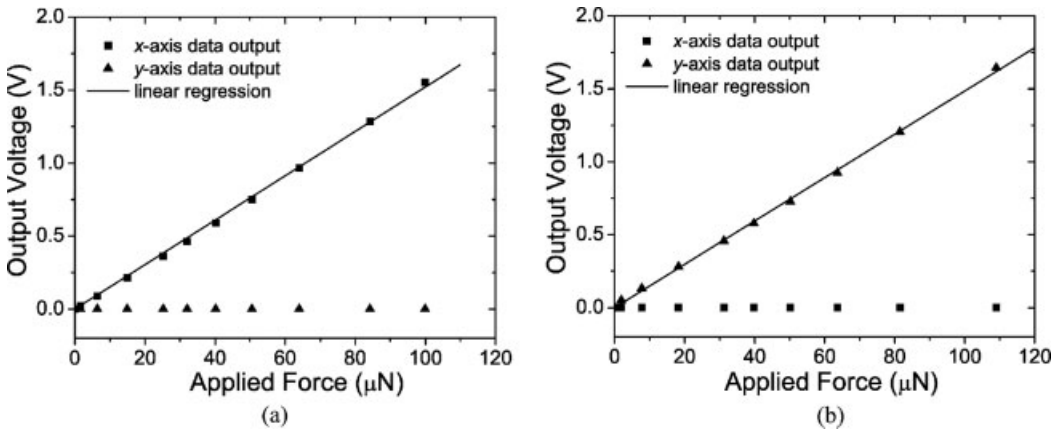

Figure 3. Sensor calibration results. (a) Forces applied along x direction. (b) Forces applied along y direction. Also shown in (a) and (b) are cross-axis data.

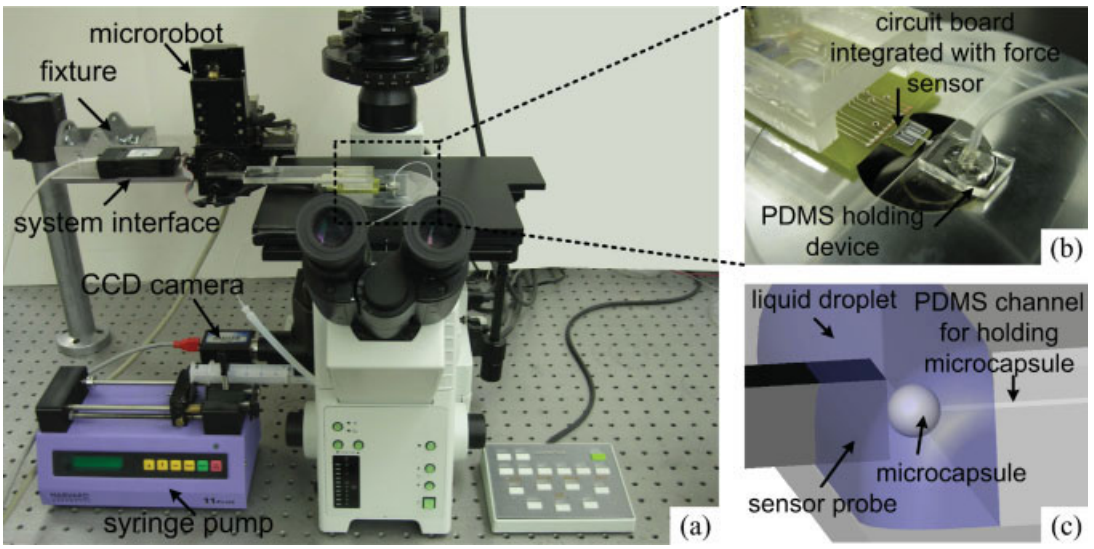

Figure 4. (a) System setup. (b) Zoom-in view of the force sensor on a circuit board approaching a PDMS microcapsule holding device. (c) 3D schematic of experimental configuration. [Color figure can be viewed in the online issue, which is available at www.interscience.wiley.com.]

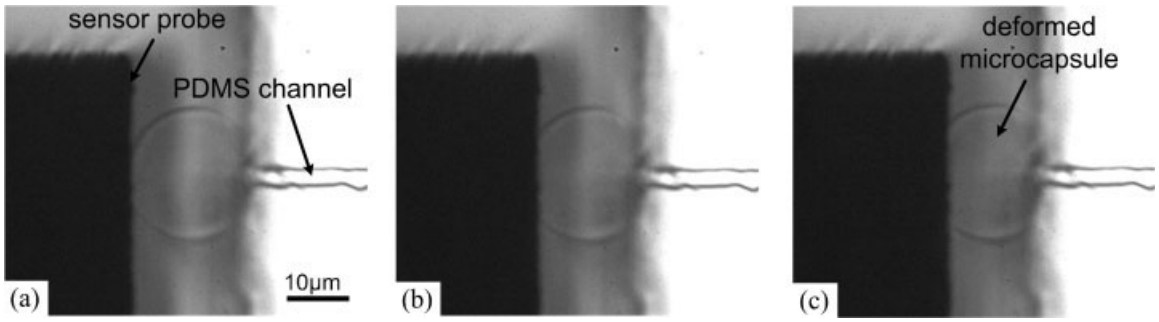

Figure 5. A series of snapshots for a microcapsule with 2% chitosan coating in PBS from a compression testing experiment: (a) Starting to compress the microcapsule; (b) 10% deformation at 441.34 nN; (c) 20% deformation at 992.90 nN.

The Hertzian half-space contact mechanics model has been widely used to characterize solid-like microparticles and biological cells.[10–12,15] The relationship between compressive displacement δ and force F is

$$\delta = \left[\frac{3(1-\nu^2)}{4E(R)^{1/2}}\right]^{2/3} F^{2/3} \tag{5}$$

where E is the Young's modulus of the material under compression (e.g., solid-like sphere), R is the radius of the solid sphere, and ν is Poisson's ratio which is assumed to be 0.5 for incompressible materials. Since this model is only applicable to small deformations ($\delta/R \leq 0.1$),[35] an extended mechanics model was developed to accommodate large deformations.[36] As shown in Figure 6, the extensive relationship between compressive displacement and force is

$$\delta = \frac{3(1-\nu^2)F}{4Ea} - \frac{f(a)F}{\pi E} \tag{6}$$

$$f(a) = \frac{2(1+\nu)R^2}{(a^2+4R^2)^{3/2}} + \frac{1-\nu^2}{(a^2+4R^2)^{1/2}} \tag{7}$$

where a is the radius of contact area. The second term of Eq. (5) is due to the reaction force, $-F$, and can be neglected within small deformation range ($\delta/R \leq 0.1$); thus, Eq. (5) can be derived by Eq. (6) which is generalized. It is shown that the value of compressive displacement δ calculated from Eq. (6) agrees better than the value calculated from Eq. (5) of Hertz theory with the experimental data for a rubber sphere in the range $\delta/R \leq 0.2$. Above this range, the values of δ become much larger than experimental results mainly because of the nonlinear elasticity of rubber.[36] Therefore, we chose 20% deformation ($\delta/R \leq 0.2$) including an extensive term from the reaction force to assess the reasonable global mechanical properties of the microcapsules and minimize the nonlinear effect, such as volume changes due to the drainage of liquid medium during compression. Assuming that the lateral extension is not significant within 20% deformation, as shown Figure 6, the radius of contact area ($0 < a < R$) as a function of compressive displacement δ can be geometrically calculated as

$$a = (R-\delta)\ \tan\theta \quad \text{and} \quad \theta = \cos^{-1}\left(\frac{R-\delta}{R}\right) \tag{8}$$

It is verified that the contact area obtained from Eq. (8) and measured from experimental images within 20% deformation are in agreement (differences < 5%).

The force–displacement curves collected on five microcapsules of each type [Fig. 7(a–c)] in DDI water were nonlinear least squares curve fitted with Eq. (6), as shown in Figure 7(d), for determining Young's modulus values. As shown in Figure 9(a), the Young's modulus values of the microcapsules in DDI water were 143.00 ± 32.88, 354.31 ± 33.705, and 458.66 ± 83.50 kPa, for 1, 2, and 3% chitosan-coated microcapsules, respectively. It is shown that the

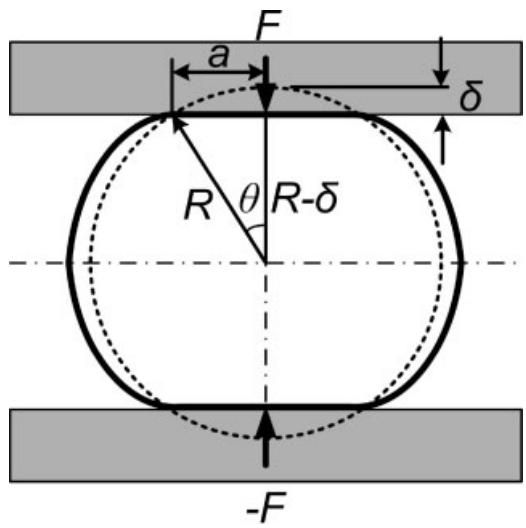

Figure 6. Schematic of a large elastic deformation model for characterizing Young's modulus.

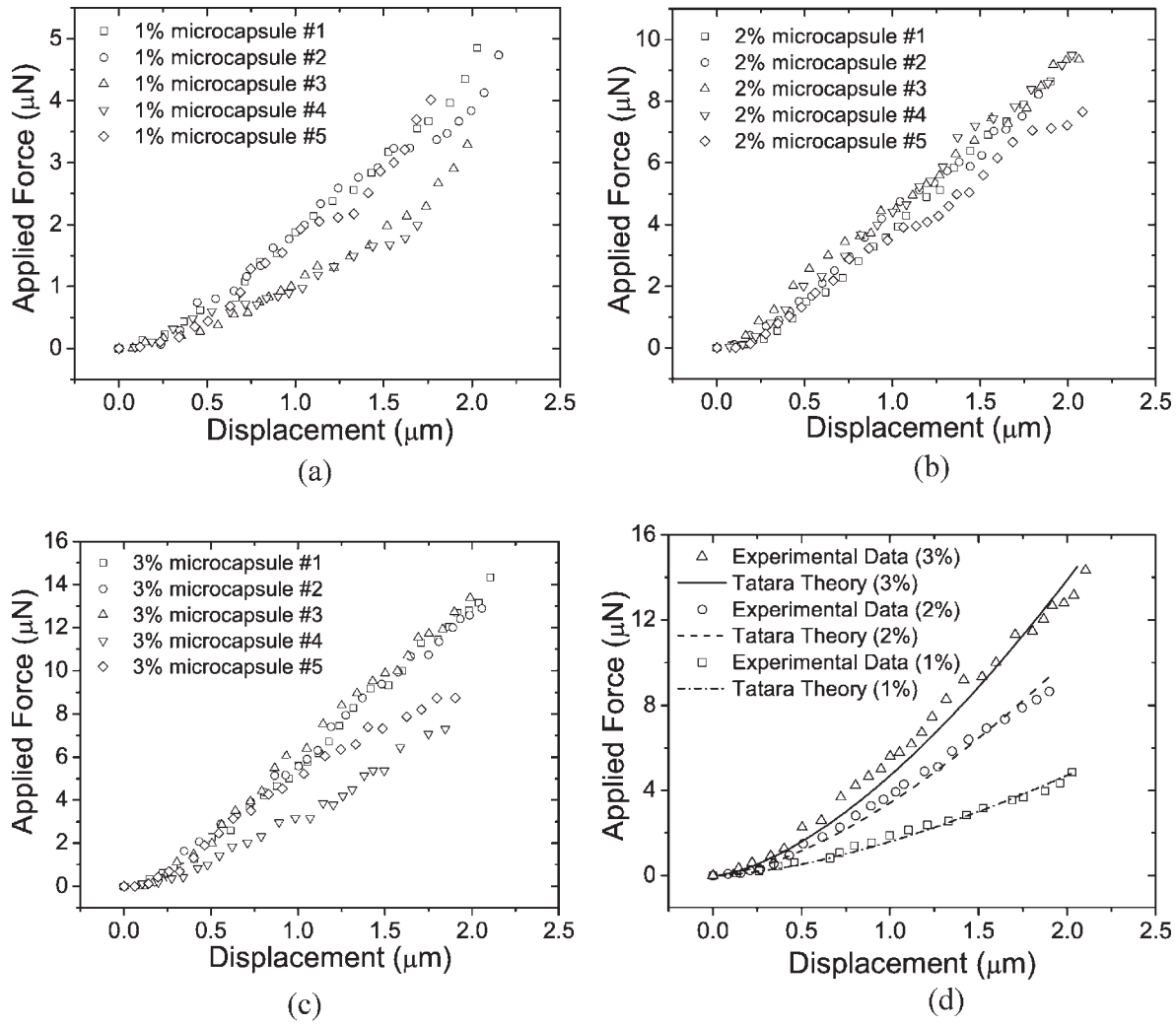

Figure 7. Force–displacement curves for (a) 1% chitosan-coated alginate microcapsules, (b) 2% chitosan-coated microcapsules, and (c) 3% chitosan-coated microcapsules in DDI water. (d) Representative force–displacement curves fitted with large deformation mechanics model for each 1, 2, and 3% chitosan-coated microcapsules, respectively.

change of chitosan concentration from 1 to 2% significantly increases the stiffness of the microcapsules in DDI water, but the change from 2 to 3% has less influence on stiffness increase.

To investigate the physiological effect and the relationship between the mechanical properties and drug release kinetics of the microcapsules in a simulated *in vivo* environment, microscale compression testing in pH 7.4 PBS was also conducted. Figure 8(a–c) shows the force–displacement curves of 1, 2, and 3% chitosan-coated microcapsules in PBS. Figure 8(d) shows representative fitted curves. The obtained Young's modulus values shown in Figure 9(b) were 11.87 ± 4.94, 32.69 ± 11.40, and 42.83 ± 14.48 kPa, for 1, 2, and 3% chitosan-coated microcapsules, respectively, which are comparable to Young's modulus of human erythrocytes (red blood cells), 26 ± 7 kPa.[3] This result indicates that the microcapsules at the physiological pH (i.e., pH 7.4) can be made as soft/deformable as blood cells and thus may be mechanically suitable for intravenous injection use if they are made with the size of blood cells (e.g., 4–10 μm in diameter).

Protein release kinetics

The kinetics of GOx release from the microcapsules coated with various chitosan solutions was tested at 37°C in pH 7.4 PBS and DDI water separately. Figure 10(a) shows that the rate of GOx release in PBS decreases as the chitosan concentration increases from 1 to 3%. In 8 h, there are 3.4, 2.3, and 1.2% of loaded GOx released from the microcapsules coated with 1, 2, and 3% chitosan, respectively. In DDI water, however, the microcapsules are much

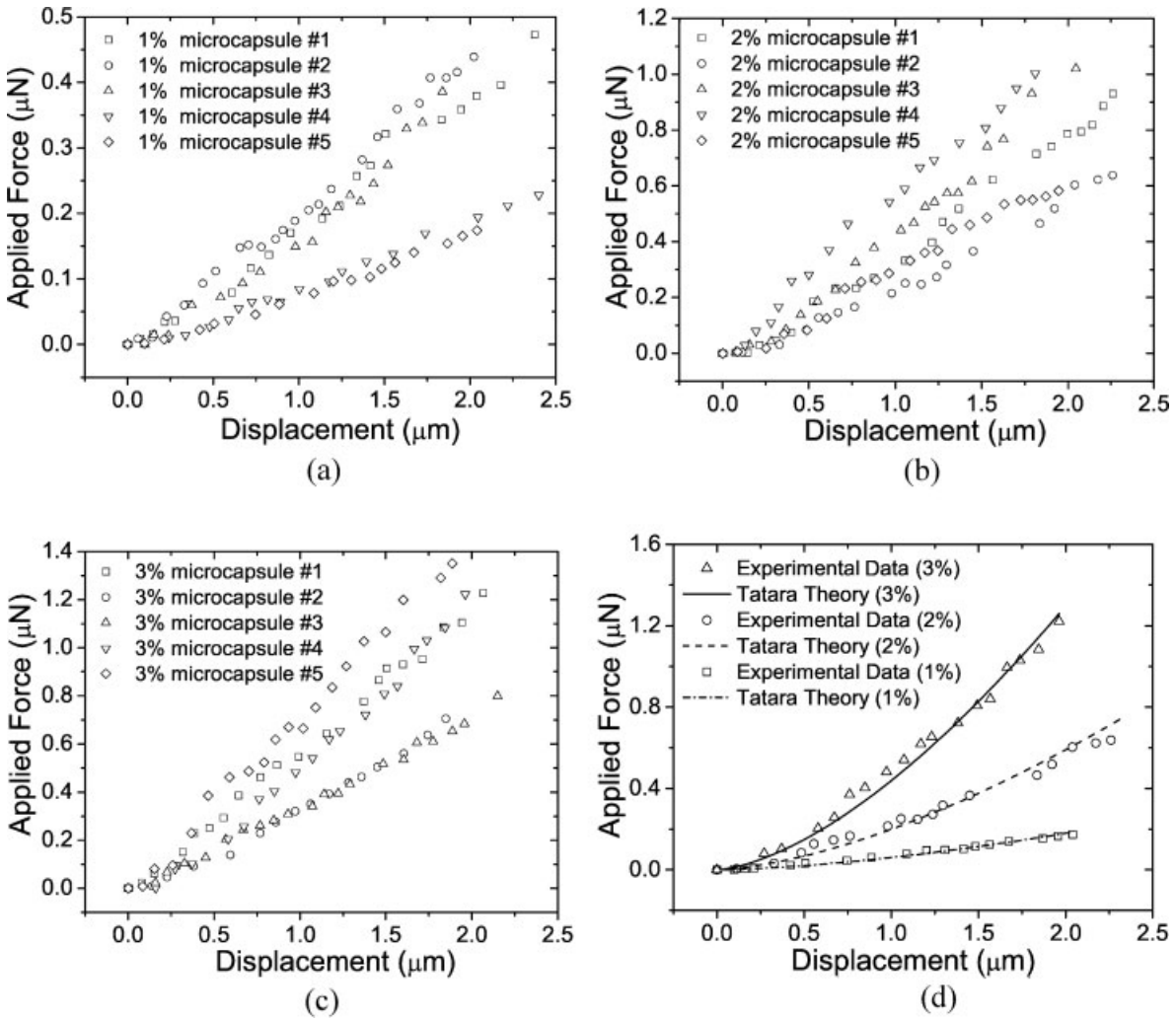

Figure 8. Force–displacement curves for (a) 1% chitosan-coated alginate microcapsules, (b) 2% chitosan-coated microcapsules, and (c) 3% chitosan-coated microcapsules in pH 7.4 PBS. (d) Representative force–displacement curves fitted with large deformation mechanics model for 1, 2, and 3% chitosan-coated microcapsules, respectively.

less permeable, with about 0.05% of GOx released, regardless of chitosan concentration in the coating solution [Fig. 10(b)].

The slower GOx release in DDI water might be caused by lower pH and lower electrolyte concentration, which affect the binding of alginate with chitosan and with calcium ions. Chitosan consists of primary amino groups that have pK_a values of about 6.3 and alginate has pK_a values of 3.2 to 3.4. In DDI water of pH 6.3, about 50% of the amino groups are protonized, which can form strong complexes with the carboxylic groups in alginate that are also ionized. In pH 7.4 PBS, the ionization degree of amino groups decreases; in the meantime, the monovalent K^+ and Na^+ ions can exchange with Ca^{2+} that initially formed cross-links with alginate, $Ca^{2+}(—COOH)_2$, converting the cross-linked gel to soluble polymer chains. The presence of small electrolytes can also weaken the binding of polyelectrolytes of opposite charges. As a result, the cross-linking density of the microcapsules is reduced, leading to approximately 11-fold decrease in Young's modulus and an increase in the release rate.

The pH- and ionic strength-dependent protein release kinetics presents an advantage of the alginate–chitosan microcapsules for biomedical applications. The protein-loaded microcapsules can be stored in a salt-free medium of weakly acidic pH with negligible release. Upon administered *in vivo*, the encapsulated protein would start to release in the physiological fluid.

Correlation between protein release kinetics and mechanical properties

As an attempt to correlate the protein release kinetics with mechanical properties, the percent of GOx released in pH 7.4 PBS at 3, 5, and 8 h was

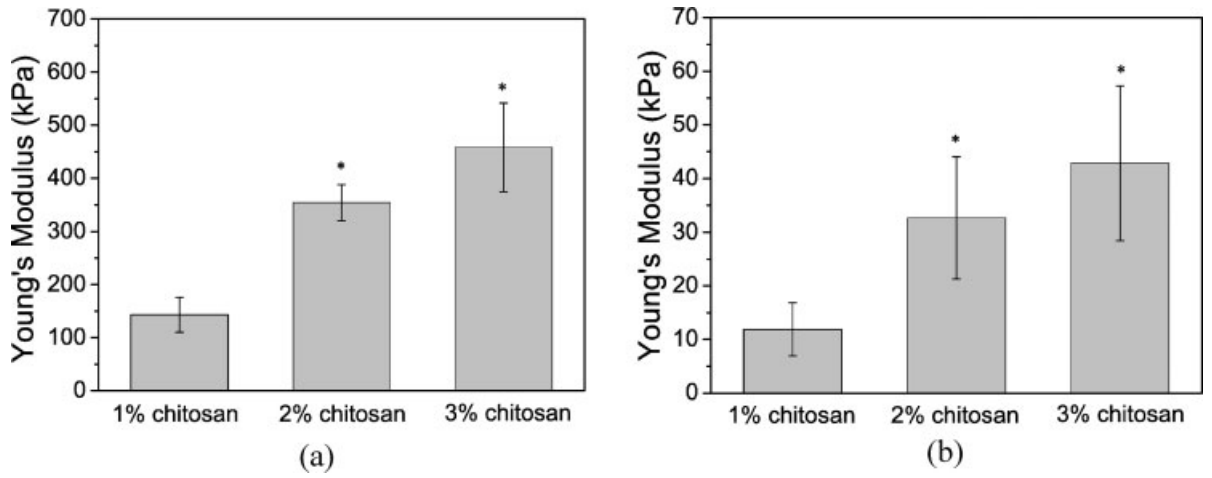

Figure 9. Young's modulus values of microcapsules with different percentages of chitosan coating in (a) DDI water and (b) pH 7.4 PBS. The data points and the error bars represent means ± SD ($n = 5$). Asterisk (*) indicates significant differences from the value at 1% of chitosan concentration ($p < 0.05$).

plotted against the Young's modulus of the microcapsules in Figure 10(c) using the data in Figures 9(b) and 10(a). It can be seen that as the Young's modulus increases from 12 kPa (for 1% chitosan-coated microcapsules) to 43 kPa (for 3% chitosan-coated microcapsules), the percent of released GOx decreases about 1.8-fold at 5 h and 1.9-fold at 8 h. This result suggests an existence of a correlation between the protein release rate and Young's modulus of the microcapsules. While finding the upper bound of the Young's modulus for GOx release requires more extensive tests, it may be speculated that the release of a protein from the microcapsules is trivial when the Young's modulus is over 200 kDa based on the data collected from the microcapsules in DDI water [Figs. 9(a) and 10(b)]. At a high Young's modulus, the alginate–chitosan hydrogel microcapsules may be too dense to allow a protein such as GOx to diffuse out, with a molecular weight of 160 kDa and molecular size about 14 nm × 10 nm.[37]

Solute diffusion in a hydrogel depends on the swelling degree of the hydrogel, which is in turn a function of cross-linking density or mesh size of the networks. As discussed earlier, in pH 7.4 PBS, the cross-linking density of the microcapsules may be lowered because of the dissociation of the polymer complexes and $Ca^{2+}(COOH)_2$ cross-links as well as ionization of alginate. Conceivably the swelling degree of the microcapsules is higher in pH 7.4 PBS than in DDI water, so is the solute diffusion coefficient according to the free volume theory by Yasuda's equation.[38] The actual dependence of swelling degree of the microcapsules on pH and salt concentration, however, remains to be determined. For bulk hydrogels, their hydration degree is normally evaluated from the weight gain after swelling equilibration. For hydrogel microparticles, the accurate measurement of equilibrium hydration is difficult because of their small dimension and huge specific surface area. It is virtually impossible to differentiate the interstitial surface among the microparticles from that inside the microparticles, which introduces large errors in the determination of hydration degree of the microparticles.

In contrast, the MEMS force sensing system presented in this article is able to determine the mechanical parameters of individual microparticles. If these mechanical parameters can be correlated with water content of the microparticles, one can predict solute diffusivity based on the free volume theory and thereafter the solute release kinetics.[39,40] Hence, it is worth further investigating the quantitative correlation between the mechanical parameters quantified by the MEMS method and hydration degree of hydrogel microcapsules.

CONCLUSION

This article presents a study of the mechanical properties of alginate–chitosan microcapsules in relation with protein release kinetics. A MEMS capacitive force sensor with a 33.2 nN force resolution provides a flexible microscale compression testing platform for characterizing mechanical properties of biomaterials. The force sensors were applied to compressing alginate microcapsules with 1, 2, and 3% chitosan coating. Based on collected force–displacement data, Young's modulus values were determined with a large elastic deformation model. The stiffness of the microcapsules in PBS was found comparable to human erythrocytes. The characterization results quantitatively reveal the effect of chitosan coating on the mechanical properties of the

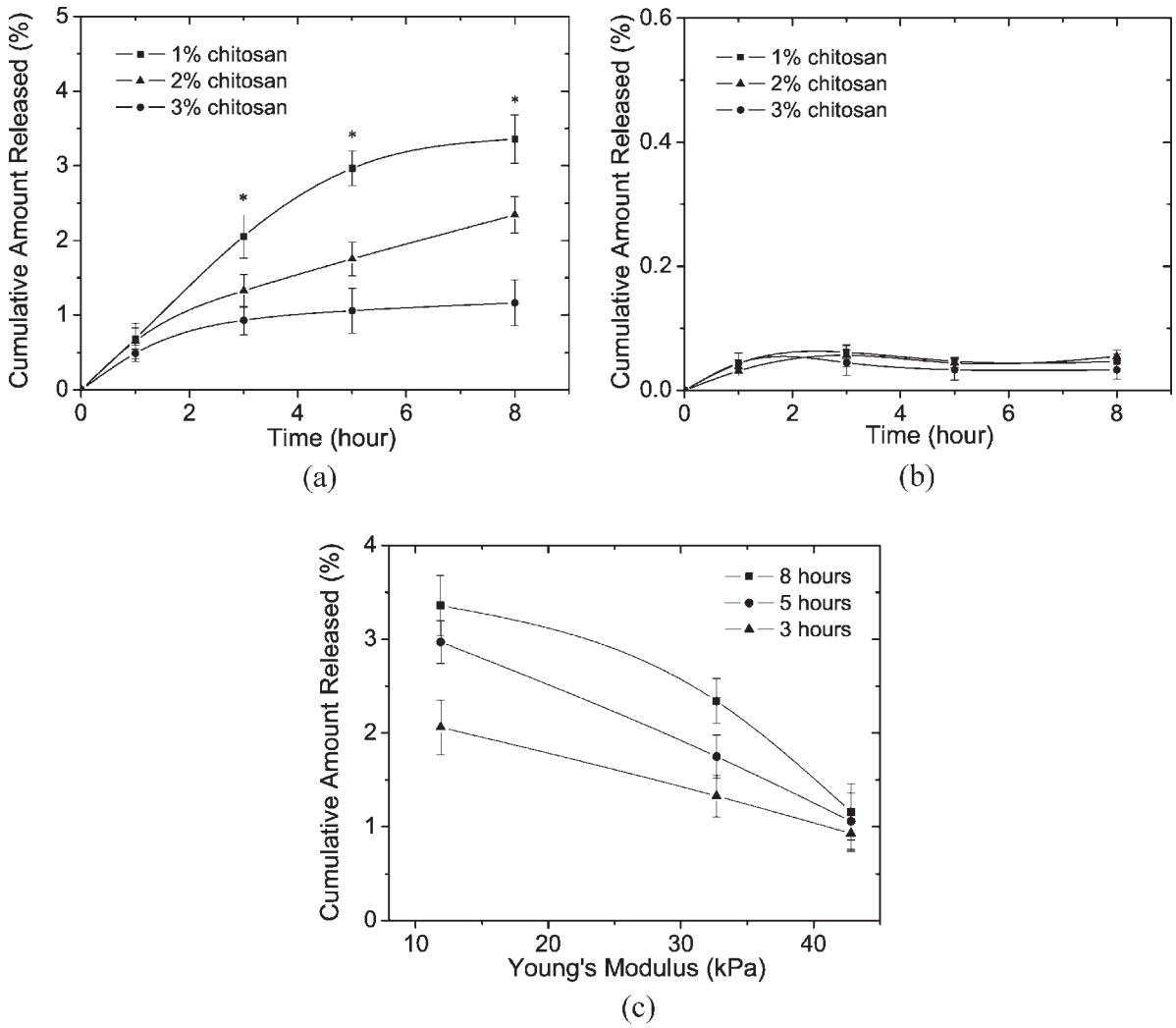

Figure 10. Kinetics of GOx release from the GOX-loaded microcapsules at 37°C in (a) pH 7.4 PBS and (b) DDI water. (c) Correlation between the cumulative amounts of GOx released at various times as a function of Young's modulus of the microcapsules in pH 7.4 PBS. GOx was loaded by incubating 0.5 mL of alginate–chitosan microcapsules in 0.5 mL of 0.5 mg/mL GOx in pH 4 buffer and then coated with chitosan solutions of different concentrations. The data points and error bars represent mean ± SD ($n = 3$). In Figure 9(c), asterisk (*) indicates significant differences from the value at 1% of chitosan concentration ($p < 0.05$). The similarity factor f_1 recommended by FDA (Food and Drug Administration, USA) was also calculated for the time-course curves in pH 7.4 PBS. The f_1 values ranged from 33 to 60, all greater than 15, indicating that the use of 1, 2, and 3% chitosan solutions resulted in different release curves.

microcapsules. The release tests demonstrated that faster protein release occurred in pH 7.4 PBS than in DDI water. In correlation between drug release rate and mechanical properties, stiffer microcapsules showed lower drug release rates, quantitatively demonstrating that chitosan coating significantly affects protein release profiles and the mechanical properties of alginate microcapsules.

References

1. Hochmuth RM. Micropipette aspiration for living cells. J Biomech 2000;33:15–22.
2. Vinckier A, Semenza G. Measuring elasticity of biological materials by atomic force microscopy. FEBS Lett 1998;430:12–16.
3. Dulinska I, Targosz M, Strojny W, Lekka M. Czuba P, Balwierz W, Szymonski M. Stiffness of normal and pathological erythrocytes studied by means of atomic force microscopy. J Biochem Biophys Methods 2006;66:1–11.
4. Bausch AR, Moller W, Sackmann E. Measurement of local viscoelasticity and force in living cells by magnetic tweezers. Biophys J 1999;76:573–579.
5. Zhang Z, Ferenczi MA, Thomas CR. A micromanipulation technique with a theoretical cell model for determining mechanical properties of single mammalian cells. Chem Eng Sci 1992;47:1347–1354.
6. Blewett J, Burrows K, Thomas C. A micromanipulation method to measure the mechanical properties of single tomato suspension cells. Biotech Lett 2000;22:1877–1883.
7. Smith AE, Zhang Z, Thomas CR, Moxham KE, Middelberg APJ. The mechanical properties of *Saccharomyces cerevisiae*. PNAS 2000;97:9871–9874.

8. Liu KK, Williams DR, Briscoe BJ. Compressive deformation of a single microcapsule. Phys Rev E 1996;54:6673–6680.
9. Zhang Z, Saunders R, Thomas CR. Mechanical strength of single microcapsule determined by a novel micromanipulation technique. J Microencapsul 1999;16:117–124.
10. Wang CX, Cowen C, Zhang Z, Thomas CR. High-speed compression of single alginate microspheres. Chem Eng Sci 2005;60:6649–6657.
11. Chan V, Liu KK, Le Visage C, Ju B-F, Leong KW. Bioadhesive characterization of poly (methylidene malonate 2.12) microparticle on model extracelluar matrix. Biomaterials 2004;25:4327–4332.
12. Ding P, Norton IT, Zhang Z, Pacek AW. Mechanical properties of gelatine-rich micro-particles. J Food Eng 2008;86:307–314.
13. Lulevich VV, Andrienko D, Vinogradova OI. Elasticity of polyelectrolyte multilayer microcapsules. J Chem Phys 2004;120: 3822–3826.
14. Lulevich VV, Vinogradova OI. Effect of pH and salt on the stiffness of polyelectrolyte multilayer microcapsules. Langmuir 2004;20:2874–2878.
15. Lulevich VV, Zink T, Chen H-Y, Liu F-T, Liu G-Y. Cell mechanics using atomic force microscopy-based single-cell compression. Langmuir 2006;22:8151–8155.
16. Lin G, Palmer RE, Pister KSJ, Roos KP. Miniature heart cell force transducer system implanted in MEMS technology. IEEE Trans Biomed Eng 2001;48:996–1006.
17. Zhang XJ, Zappe S, Bernstein RW, Sahin O, Chena C-C, Fish M, Scott MP, Solgaard O. Micromachined silicon force sensor based on diffractive optical encoders for characterization of microinjection. Sensor Actuat A 2004;114:197–203.
18. Yang S, Saif T. Micromachined force sensors for the study of cell mechanics. Rev Sci Instrum 2005;76:044301.
19. Zhao Y, Zhang X. Cellular mechanics study in cardiac myocytes using PDMS pillars array. Sensor Actuat A 2006;125:398–404.
20. Sun Y, Wan K-T, Roberts KP, Bischof JC, Nelson BJ. Mechanical property characterization of mouse zona pellucida. IEEE Trans Nanobioscience 2003;2:279–286.
21. Sun Y, Fry SN, Potasek DP, Bell DJ, Nelson BJ. Characterization fruit fly behavior using a microforce sensor with a new comb-drive configuration. J Microelectromech Syst 2005;14:4–11.
22. Liu Q, Rauth AM, Wu XY. Immobilization and bioactivity of glucose oxidase in hydrogel microspheres formulated by an emulsification-internal gelation-adsorption-polyelectrolyte coating method. Int J Pharm 2007;339:148–156.
23. Lim F, Sun AM. Microencapsulated islets as bioartificial endocrine pancreas. Science 1980;210:908–910.
24. Hisano N, Morikawa N, Iwata H, Kada Y. Entrapment of islets into reversible disulfide hydrogel. J Biomed Mater Res 1998;40:115–123.
25. Hearn E, Neufeld RJ. Poly (methylene *co*-guanidine) coated alginate as an encapsulation matrix for urease. Proc Biochem 2000;35:1253–1260.
26. Bowersock TL, Hogenesch H, Suckow M, Guimond P, Martin S, Borie D, Torregrosa S, Park H, Park K. Oral vaccination of animals with antigens encapsulated in alginate microspheres. Vaccine 1999;17:1804–1811.
27. Hari PR, Chandy T, Sharma CP. Chitosan/calcium-alginate beads for oral delivery of insulin. J Appl Polym Sci 1996; 59:1795–1801.
28. Mumper RJ, Hoffman AS, Puolakkainen P, Bouchard LS, Gombotz WR. Calcium-alginate beads for the oral delivery of transforming growth factor-β_1: Stabilization of TGF-β_1 by the addition of polyacrylic acid within acid-treated beads. J Control Release 1994;30:241–251.
29. Gu F, Amsden B, Neufeld R. Sustained delivery of vascular endothelial growth factor with alginate beads. J Control Release 2004;96:463–472.
30. Polk A, Amsden B, Yao KD, Peng T, Goosen MFA. Controlled release of albumin from chitosan-alginate microcapsules. J Pharm Sci 1994;83:178–185.
31. Liu LS, Liu SQ, Ng SY, Froix M, Ohno T, Heller J. Controlled release of interleukin-2 for tumor immunotherapy using alginate/chitosan porous microspheres. J Control Release 1997; 43:65–74.
32. Lee JE, Kim KE, Kwon IC, Ahn HJ, Lee SH, Cho H, Kim HJ, Seong SC, Lee MC. Effects of the controlled-released TGF-beta 1 from chitosan microspheres on chondrocytes cultured in a collagen/chitosan/glycosaminoglycan scaffold. Biomaterials 2004;25:4163–173.
33. Wang SB, Chen AZ, Weng LJ, Chen MY, Xie XL. Effect of drug-loading methods on drug load, encapsulation efficiency and release properties of alginate/poly-L-arginine/chitosan ternary complex microcapsules. Macromol Biosci 2004;4:27–30.
34. Sun Y, Nelson BJ, Potasek DP, Enikov E. A bulkmicrofabricated multi-axis capacitive cellular force sensor using transverse comb drives. J Micromech Microeng 2002;12:832–840.
35. Liu KK. Deformation behaviour of soft particles: A review. J Phys D: Appl Phys 2006;39:R189–R199.
36. Tatara Y. Large deformations of a rubber sphere under diametral compression (Part 1: Theoretical analysis of press approach, contact radius and lateral extension). J Soc Mech Eng Ser A 1993;36:190–196.
37. Otsuka I, Yaoita M, Seiichi N, Higano M. Molecular dimensions of dried glucose oxidase on a Au(1 1 1) surface studied by dynamic mode scanning force microscopy. Electrochim Acta 2005;50:4861–4867.
38. Yasuda H, Peterlin A, Colton CK, Smith KA, Merrill EW. Permeability of solutes through hydrated polymer membranes. Part III. Die Makromol Chem 1969;126:177–186.
39. Abdekhodaie MJ, Wu XY. Drug release from ion-exchange microspheres: Mathematical modeling and experimental verification. Biomaterials 2008;29:1654–1663.
40. Zhou Y, Chu JS, Zhou T, Wu XY. Modeling of drug release from two-dimensional matrix tablets with anisotropic properties. Biomaterials 2004;26:945–952.